PHYSICAL REVIEW B VOLUME 43, NUMBER 9 15 MARCH 1991-II

Atomic-size effects on the growth of SrF_2 and $(Ca,Sr)F_2$ on Si(111)

J. D. Denlinger, Marjorie A. Olmstead,* and Eli Rotenberg
Department of Physics, University of California, Berkeley, California 94720

J. R. Patel and E. Fontes
AT&T Bell Laboratories, Murray Hill, New Jersey 07974

(Received 24 September 1990)

Strain-induced lattice relaxation during overlayer growth is investigated by *in situ* monitoring of SrF_2 and $Ca_xSr_{1-x}F_2$ growth on Si(111) with x-ray standing-wave fluorescence and low-energy electron diffraction. Submonolayer films show both intrinsic lateral disorder and variable interface stoichiometry with discommensuration parallel to the surface after completion of the first monolayer. In contrast, local commensuration is observed for Ca-rich alloy films. In the alloy, Sr and Ca occupy different sites in the first monolayer, but have similar average positions in subsequent layers.

Epitaxial ionic insulator growth on semiconductor surfaces has attracted attention for nearly a decade due to scientific interest in interface formation between very dissimilar materials as well as to potential applications to three dimensional integrated circuitry.[1] The growth of CaF_2, SrF_2, and their alloys on Si substrates is well suited to study the role of lattice mismatch in epitaxial growth, as the room-temperature mismatch can be varied by an order of magnitude, between 0.6% and 6.8% for CaF_2 and SrF_2, respectively, while other factors which determine interface structure, such as chemical bonding energies, do not change dramatically. Photoemission studies on ultrathin (<10 Å) films have shown that the bonding and charge transfer in the first monolayer at the SrF_2/Si(111) interface is very similar to that at the CaF_2/Si(111) interface,[2] raising the question of when the strain energies implicit in such a large lattice mismatch drive the overlayer to alter its structure.

Fluoride films of high crystalline quality with crystal axes rotated 180° relative to the Si(111) substrate can be grown for both CaF_2 and SrF_2.[3] Electron micrographs of CaF_2/Si(111) show a locally commensurate interface with misfit dislocations,[4] and a tensile strain observed parallel to the interface in ion channeling has been attributed to the large thermal-expansion-coefficient mismatch.[5] The CaF_2/Si(111) interface structure for submonolayer coverages has been characterized with ion scattering[6] and x-ray standing waves,[7] which find Ca positions similar to the local structure in $CaSi_2$. The former determined Ca to bond exclusively above the second-layer Si atom (T_4 site), whereas the latter found Ca additionally to occupy sites above fourth-layer Si atoms (H_3 site).

In this study, we employ x-ray standing-wave (XSW) fluorescence in combination with low-energy electron diffraction (LEED) to investigate the growth of the first few monolayers of SrF_2 and $Ca_xSr_{1-x}F_2$ on Si(111). We find that similar to Ca, Sr does not populate a unique site for submonolayer coverages. However, discommensuration with the substrate begins at completion of the first SrF_2 monolayer, in contrast to the locally commensurate interface found for CaF_2 and $Ca_xSr_{1-x}F_2$-alloy films. Tetragonal distortion of the SrF_2 overlayer is observed, revealing an origin similar to the lateral tensile strain seen in CaF_2 growth.

For $Ca_xSr_{1-x}F_2$-alloy films ($x=0.6$–0.8), we find that the Ca and Sr atoms in the first monolayer are not equivalent, but occupy the same positions relative to the substrate as in pure CaF_2 and SrF_2; the average Sr and Ca positions are nearly the same in subsequent overlayers, similar to bulk results on other tertiary alloys.[8,9]

The XSW technique[10] is capable of locating atoms at a surface with respect to bulk-substrate Bragg planes to within $\leq 1\%$ of the diffraction-plane spacing. Upon Bragg reflection by the substrate, incident and scattered x rays interfere and form a standing-wave electric field with the periodicity of the diffracting planes and a phase with respect to the planes that varies by π as the Bragg condition is traversed. This phase variation is exploited to determine the position P of adsorbed atoms relative to the bulk Bragg planes (modulo planar spacing d_{hkl}) by monitoring its fluorescence yield, which is proportional to the standing-wave field magnitude. In addition, the modulation amplitude is related to a coherent-fraction parameter F that is reduced from unity by multiple coherent sites or random disorder of the atomic positions.

The experiments were performed at the National Synchrotron Light Source (NSLS) (AT&T beamline X15A) in an UHV system (base pressure 2×10^{-10} Torr) consisting of separate chambers for growth, for x-ray measurements, and for LEED and Auger-electron-spectroscopy (AES) analyses, with UHV transfer between them.[11] Both (111) and (220) (35.3° sample tilt) Bragg reflections were measured to give complete positional information. Photon energies near 17.5 keV were used to excite the Sr $K\alpha$ fluorescence at 14.1 keV, and 12-keV photons were used to excite the Ca $K\alpha$ fluorescence at 3.7 keV. Detection of fluorine fluorescence was not possible due to its low energy.

Well-oriented, polished (111) silicon crystals were chemically cleaned using the Shiraki etch.[12] Subsequent annealing at ~850 °C for ~10 min in UHV produced sharp 7×7 LEED patterns and no detectable impurities in the Auger spectra. SrF_2 and CaF_2 were grown from separate effusion ovens at 1300 °C onto the Si(111)7×7

substrates which were held at ~700–730 °C. The deposition rate was 1–3 monolayers (ML) per minute. Because of the sensitivity of fluorides to charged particle beams,[13] LEED and AES measurements were only taken after the x-ray analysis. The fluoride coverage was determined by Rutherford backscattering (RBS) from the Sr and Ca atoms after removal of the samples from UHV.

To understand the initial template for thick-film growth, we discuss first an 0.7-ML deposition of SrF_2 (1 ML=7.84×10^{14} atoms/cm^2), which exhibited a multidomain 5×1 LEED pattern. The x-ray reflectivity and Sr fluorescence yield for this submonolayer growth is shown in Fig. 1. A fit of the (111)-reflection data [Fig. 1(a)] gives a position value of $P_{111}=0.953\pm0.005$ ($\times d_{111}=2.99\pm0.02$ Å) above the top-layer (111) plane referenced to bulk silicon, and a coherent fraction of $F_{111}=0.77\pm0.02$. A fit of the (220) data [Fig. 1(b)] yielded values of $P_{220}=0.70\pm0.01$ ($\times d_{220}=1.33\pm0.02$ Å) and $F_{220}=0.46\pm0.03$. Triangulation of the two position values yields an apparent position near the H_3 site above the silicon surface (see inset of Fig. 1); however, multiple sites are required to explain the coherent-fraction values of less than unity.

To model the submonolayer results, we restrict the Sr atoms to the three threefold high-symmetry sites above the (111) surface. Using Sr-Si bond lengths found in $SrSi_2$ of 3.2–3.4 Å,[14] we can calculate a range of expected (111) and (220) positions for each site. For Sr bonding directly above a top-layer silicon atom (top site) we would expect $P_{111}\sim1.18$ and $P_{220}\sim0.41$. Approximately the same (111) position of ~0.91 is expected for the H_3 and T_4 bonding sites with different corresponding (220) positions of $P_{220}\sim0.71$ for H_3 and $P_{220}\sim0.37$ for T_4. Using the experimental (111) position of 0.95 in the latter two sites, a ratio of H_3 to T_4 sites equal to 70:30 agrees with the measured (220) value of 0.70 and predicts a reduced (220) coherent fraction of 60%. Here we note that in a previous XSW study of CaF_2/Si(111),[7] an equal mixture of H_3 and T_4 sites were determined to be occupied. Also, in the case of silicides, $CaSi_2$ is composed of Ca layers alternately residing in H_3 and T_4 sites between Si double layers,[15] whereas $SrSi_2$ has a different bulk structure.[14]

The simplest explanation of the reduced (111) coherent fraction is that 23% of the Sr atoms are randomly disordered, with the remainder in coherent H_3 and T_4 sites. Adding this assumption to the above model yields the experimental coherent fractions. However, an extremely rough Si substrate would be needed to allow 23% random disorder *perpendicular* to the interface for a submonolayer coverage. An alternate explanation is that multiple coherent Sr positions exist in the [111] direction. This would be the case if some fluorine was still trapped at the interface, as evidenced by a small fraction of Si-F bonding in photoemission of SrF_2/Si(111) for the same growth temperature.[2] If ~15% of the Sr atoms are placed further from the interface at a position of $P_{111}=1.20\pm0.05$ *above* the T_4 site ($P_{220}=0.77\pm0.06$, see Fig. 2) while the remainder are at $P_{111}=0.92$ above H_3 (50%) and T_4 (35%), good agreement with both (111) and (220) data can be achieved. A value of 1.2 for P_{111} for the Sr-F-Si case can be physically accounted for assuming a 1.6-Å Si-F bond length (from SiH_3F), an ionic radius of Sr in the +1 state (rather than the +2 state), and a 0.125-Å outward relaxation of the top Si layer as proposed for CaF_2/Si(111).[6] A combination of these two effects of disorder and undissociated fluorine can also explain the data.

Relative to the submonolayer sample, a growth of 1.2

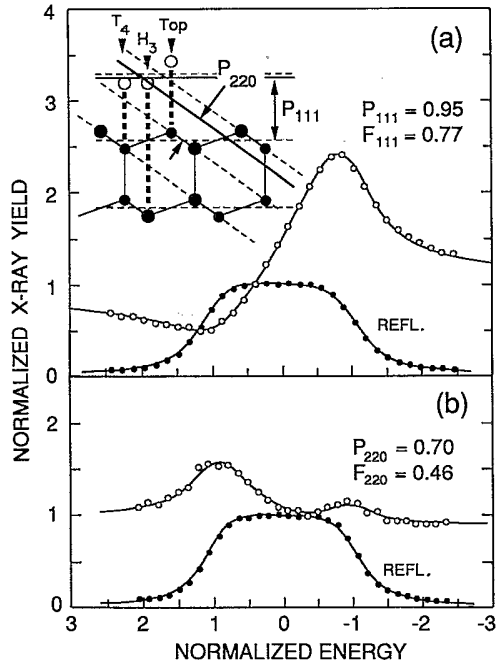

FIG. 1. Reflectivity and Sr $K\alpha$ fluorescence for 0.7 ML of SrF_2 on Si(111) using 17.5-keV incident x rays diffracting from (a) (111) substrate planes and (b) (220) planes. Solid lines are fits to the dynamical theory. Reflectivity widths are ~2.3 and ~1.0 eV, respectively. The inset illustrates triangulation of the (111) and (220) positions in comparison to the three high-symmetry Sr-Si bonding sites ($SrSi_2$ bond lengths assumed).

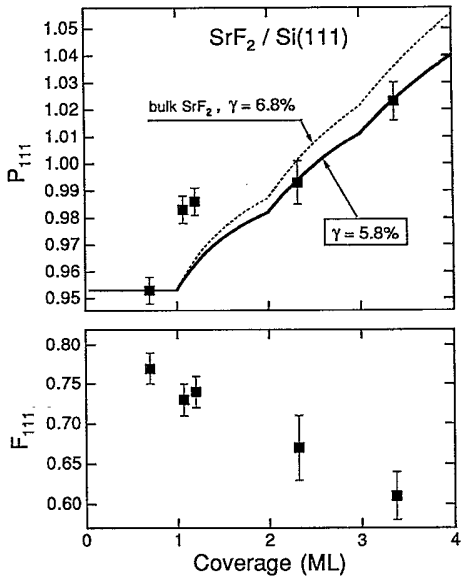

FIG. 2. Summary of (111) XSW data for SrF_2/Si(111). The solid curve, a fit to Eq. (1), shows a 1% contraction relative to bulk SrF_2 (dashed curve) at room temperature.

ML (sample C in Table I) showed a small expansion in the perpendicular apparent-position parameter $P_{111}=0.987$, and a decrease in the coherent fraction $F_{111}=0.74$. Also the (220) apparent position $P_{220}=0.67\pm0.03$, only shifted slightly (from the H_3 site towards the T_4). However, the revealing change was a significant lowering of the coherent fraction, $F_{220}=0.20\pm0.04$, indicating development of a lack of lateral registry (and/or the multiplicity of sites in island growth). This incoherency with respect to the (220) diffraction planes is attributed to lateral discommensuration (either in the first monolayer or in the second layer), and is confirmed by the appearance of secondary 1×1 LEED spots with an expanded lattice parameter of $8.0\pm0.5\%$ relative to the substrate. Additional 5×1 spots were seen for this particular growth indicating the persistence of commensurate submonolayer regions, whereas a slower growth of 1.1 ML at a higher substrate temperature (sample B) resulted in more complete discommensuration of the *first* layer as evidenced by exclusive 1×1 expanded-lattice-parameter LEED spots without any 5×1 spots. XSW measurements revealed very similar perpendicular and lateral positions; however, the completely discommensurate sample (B) had a higher local lateral coherency ($F=0.33\pm0.03$) than the mixed LEED sample (C).

The expanded lattice constant seen by LEED for these very thin SrF_2 films is very close to the growth-temperature mismatch of 8.3%. This suggests that while discommensuration relieves the large compressive strain at the growth temperature, the resulting interfacial defects are completely pinned upon cooling to room temperature (RT), creating a lateral tensile strain of $1.2\pm0.5\%$ relative to the equilibrium RT mismatch of 6.8%. A similar 9% lattice-mismatch-driven discommensuration within the first 5 Å of the BaF_2/Ge(111) interface has previously been imaged using high-resolution electron microscopy.[16]

For coverages greater than 2 ML, lateral Sr-atom triangulation measurements were not attempted due to the multiplicity of interface sites and lateral discommensuration. XSW measurements on different overlayer thicknesses do, however, monitor vertical relaxation. By applying a simple model assuming an interfacial separation of δ and a constant overlayer d spacing of $1+\gamma$, the relation between the XSW fit parameters and the overlayer coverage, N (in ML), can be expressed as[17]

$$F_{111}\cos(2\pi P_{111}) = \frac{\sin(\tilde{N}\pi\gamma)}{N\sin(\pi\gamma)}\cos\left[2\pi\left(\delta+\frac{\tilde{N}-1}{2}\gamma\right)\right] + [(N-\tilde{N})/N]\cos[2\pi(\delta+\tilde{N}\gamma)], \quad (1)$$

where $\tilde{N}$ is the integer number of complete monolayers. Applying this equation to samples D and E, assuming $\delta=0.953$ from sample A, we derive $\gamma=5.8\pm0.7\%$ (see Fig. 2). The larger (111) position seen in the 1.1- and 1.2-ML samples may be due to the presence of excess fluorine trapped at the interface or to islanding. The overlayer d spacing of 1.058 relative to (111) silicon is compressed compared to the equilibrium RT mismatch of 1.068. This $1.0\pm0.7\%$ perpendicular compressive strain and the 1.2% lateral tensile strain seen by LEED are consistent with the bulk SrF_2(111) Poisson ratio of $v=0.88$.[18]

In addition to pure SrF_2 deposition, results for three mixed growths of $Ca_xSr_{1-x}F_2$ ($0.6\le x\le0.8$) are presented in Fig. 3. The single monolayer coverage yielded two distinct (111) positions of 0.89 for Ca and 0.97 for Sr, indicative of H_3 and/or T_4 bonding sites with the different cation-Si bond lengths found for the pure systems. For thicker films, the average Ca and Sr positions approach each other and become nearly identical at 10 ML (see Fig. 3). If we assume that $(Ca,Sr)F_2$ has a bimodal distribution of cation-anion bonds as seen by extended x-ray-absorption fine structure in other random solid solutions,[8,9] then our result suggests, though not conclusively, that Ca and Sr occupy a nearly undisturbed

TABLE I. Summary of sample growth and LEED analysis. Substrate temperature ~700 °C except (B,F–H)~730 °C. Deposition rate ~3 ML/min except (B,G) ~1 ML/min.

Sample	Ca coverage (ML)	Sr coverage (ML)	LEED[a]
A	0	0.7	5×1
B	0	1.08[b]	1×1, +8%
C	0	1.19[b]	5×1 and 1×1, +8%
D	0	2.27[b]	1×1, +8%
E	0	3.35[b]	1×1, +8%
F	0.9	0.2	
G	1.0	0.75	1×1
H	7.4	2.6	1×1

[a]Percentages are overlayer lattice expansion relative to bulk silicon deduced from secondary 1×1 LEED spots.
[b]RBS values corrected ($\times1.08$) for expanded overlayer lattice constant.

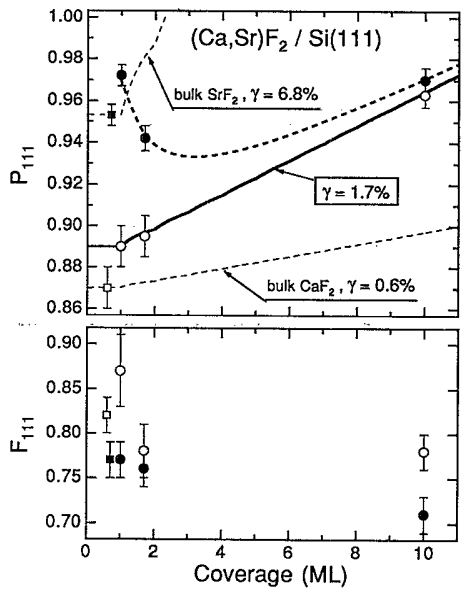

FIG. 3. Summary of (111) XSW data (○, Ca; ●, Sr) for $(Ca,Sr)F_2$/Si(111). The solid Ca curve is a fit to Eq. (1). See text for an explanation of the bold-dashed Sr curve. Also plotted are submonolayer results for pure CaF_2 (□, Ref. 7) and SrF_2 (■) with extrapolated bulk apparent positions.

bulk sublattice, whereas the fluorine sublattice distorts to accommodate two different bond lengths.

The contrast in linear and nonlinear behavior of the Ca and Sr P_{111} data can be explained by the Ca-rich stoichiometry of the films. Applying the overlayer model [Eq. (1)] to the Ca(111) positions, we derive $\gamma = 1.7 \pm 0.2\%$. Assuming Vegard's law, a $Ca_{0.75}Sr_{0.25}F_2$ film has a 2.2% (3.7%) lattice mismatch to silicon at room (growth) temperature. Hence the 10-ML mixed fluoride film is compressed along [111] by 0.5% and, assuming elastic deformation ($\nu \sim 0.88$–0.96), has a planar tensile strain of $\sim 0.5\%$ (not resolvable in our LEED system). This smaller tensile strain, compared to the maximum of $1.5\% (= 3.7\% - 2.2\%)$ expected for complete interfacial defect pinning, indicates significant strain relief upon cooling of the substrate. The nonlinear Sr(111) model in Fig. 3, top panel (bold-dashed curve), uses Eq. (1) with distinct Sr-Si interface bonds ($\delta = \delta_{Sr} = 0.97$) for the first layer and with overlayer Sr atoms residing above Ca interface regions ($\delta = \delta_{Ca} = 0.89$) as illustrated in Fig. 4.

Figure 3 shows the (111) coherent fraction of Ca to be consistently larger than that of Sr. This may be the result of the Ca-rich stoichiometry or may be due to the larger atomic size of Sr, causing Sr to deviate by a greater amount than Ca from high-symmetry sites near step edges or domain boundaries. Variations in sample preparation prevent the coherent fractions in Fig. 3 to be modeled by Eq. (1), but the shallower decline of the mixed fluoride F_{111} compared to pure SrF_2 (Fig. 2) is a direct result of the smaller overlayer lattice constant.

Lateral (220) measurements of the thin mixed fluoride films were also performed. Sr in sample F ($P_{220} = 0.67$, $F_{220} = 0.35$) is comparable to the submonolayer pure SrF_2 film. The low excitation cross section and low Ca coverage prevented a proper fit of the (220) Ca fluorescence modulation. For sample G, the Ca result ($P_{220} = 0.66$, $F_{220} = 0.22$) was quite distinct from Sr ($P_{220} = 0.42$, $F_{220} = 0.24$). A 1×1 LEED pattern without secondary spots indicates a locally commensurate interface. Hence the low (220) coherent fractions are due, not to discommensuration, but to the multiplicity of sites in the second layer above a double-species (Ca,Sr), double-site (H_3,T_4) interface. The Sr position agrees well with an equal mixture of H_3 and T_4 interface sites with type-B orientation and $\gamma < 2\%$ for the second-layer Sr atoms (Fig. 4).

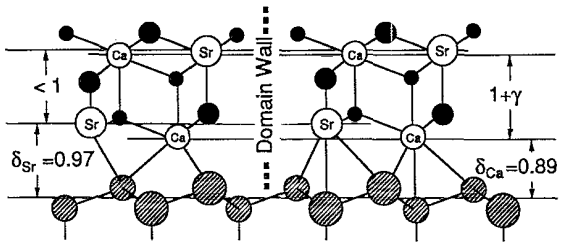

FIG. 4. A 2-ML type-B mixed fluoride overlayer diagram, showing the multiplicity of lateral and perpendicular Ca and Sr atomic sites. Solid (hatched) circles are fluorine (silicon).

In conclusion, XSW triangulation has shown the interface structure of $SrF_2Si(111)$ to consist of multiple cation bonding sites with the possibility of some interfacial fluorine for our growth temperature, similar to the case for pure $CaF_2/Si(111)$. Submonolayer coverage of a mixed fluoride exhibits distinct Ca and Sr positions simultaneously. Lateral discommensuration after completion of the first monolayer of pure SrF_2 is observed and nearly complete pinning of interfacial defects upon cooling results in large tetragonal distortion. In contrast, a locally commensurate interface and smaller tetragonal distortion is seen in Ca-rich alloy overlayers indicating significant strain relief upon cooling. Finally, distortion of the mixed cation sublattice due to the presence of our interface diminishes for thicker films.

We are grateful to R. Bringans for the loan of Knudsen cells. Work was performed at NSLS, which is supported by U.S. Department of Energy (DOE), Division of Material Sciences and Division of Chemical Sciences. J.D.D. was supported by the U.S. Department of Defense, AFOSR Contract No. F49620-87-K-0001. M.A.O. was supported by NSF Grant No. DMR-8657623. E.R. thanks the U.S. Department of Education for partial financial support.

*Present address: Department of Physics, University of Washington, Seattle, WA 98195.

[1]L. J. Schowalter and R. W. Fathauer, Crit. Rev. Solid State Mater. Sci. **15**, 367 (1989).

[2]M. A. Olmstead and R. D. Bringans, Phys. Rev. B **41**, 8420 (1990).

[3]T. Asano and H. Ishiwara, Appl. Phys. Lett. **42**, 517 (1983).

[4]F. A. Ponce *et al.*, J. Vac. Sci. Technol. B **4**, 1121 (1986); J. L. Batsone, J. M. Phillips, and E. C. Hunke, Phys. Rev. Lett. **60**, 1394 (1988).

[5]S. Hashimoto, J.-L. Peng, and W. M. Gibson, Appl. Phys. Lett. **47**, 1071 (1985).

[6]R. M. Tromp and M. C. Reuter, Phys. Rev. Lett. **61**, 1756 (1988).

[7]J. Zegenhagen and J. R. Patel, Phys. Rev. B **41**, 5315 (1990).

[8]J. C. Mikkelson, Jr. and J. B. Boyce, Phys. Rev. B **28**, 7130 (1983).

[9]A. Balzarotti *et al.*, Phys. Rev. B **30**, 2295 (1984).

[10]B. W. Batterman, Phys. Rev. **133**, A759 (1964); N. Hertel, G. Materlik, and J. Zegenhagen, Z. Phys. B **58**, 199 (1985).

[11]J. Zegenhagen *et al.*, Appl. Phys. Lett. **53**, 252 (1988).

[12]A. Ishizaka and Y. Shiraki, J. Electrochem. Soc. **133**, 666 (1986).

[13]Ch. L. Strecker, W. E. Moddeman, and J. T. Grant, J. Appl. Phys. **52**, 6921 (1981).

[14]K. Janzon, H. Schaefer, and A. Weiss, Angew. Chem. Int. Ed. Engl. **4**, 245 (1965).

[15]J. F. Morar and M. Wittmer, Phys. Rev. B **37**, 2618 (1988).

[16]J. M. Gibson and Julia M. Phillips, Appl. Phys. Lett. **43**, 828 (1983).

[17]E. Vlieg *et al.*, Surf. Sci. **178**, 36 (1986).

[18]Y. Saitoh, H. Hashizume, and K. Tsutsui, Jpn. J. Appl. Phys. **27**, 1386 (1988).